Journal of Photochemistry and Photobiology A: Chemistry 199 (2008) 23–33

Contents lists available at ScienceDirect

Journal of Photochemistry and Photobiology A: Chemistry

journal homepage: www.elsevier.com/locate/jphotochem

Study of the spectroscopic properties and first hyperpolarizabilities of disperse azo dyes derived from 2-amino-5-nitrothiazole

Antonio E.H. Machado[a,*], Newton M.B. Neto[b], Leonardo T. Ueno[a], Lucas F. de Paula[a], Diesley M.S. Araújo[a], Guedmiller S. Oliveira[a], Weverson R. Gomes[a], Rodrigo de Paula[a], Paulo L. Franzen[c], Sérgio C. Zilio[c], Ana M.F. Oliveira-Campos[d], A.M. Fonseca[d], Lígia M. Rodrigues[d], P.O. Nkeonye[d], Radim Hrdina[e]

[a] *Universidade Federal de Uberlândia, Instituto de Química, Laboratório de Fotoquímica, P.O. Box 593, Uberlândia, 38400-902 Minas Gerais, Brazil*
[b] *Instituto de Física, Universidade Federal de Uberlândia, Uberlândia, Minas Gerais, Brazil*
[c] *Instituto de Física de São Carlos, Universidade de São Paulo, São Carlos, São Paulo, Brazil*
[d] *Centro de Química, Universidade do Minho, Campus de Gualtar, Braga, Portugal*
[e] *Department of Organic Technology, Faculty of Chemical Technology, University of Pardubice, Czech Republic*

ARTICLE INFO

Article history:
Received 5 December 2007
Received in revised form 12 April 2008
Accepted 20 April 2008
Available online 29 April 2008

Keywords:
Azo dyes
Solvatochromism
EDA complexes
Fluorescence
Quantum mechanical calculations
First hyperpolarizability

ABSTRACT

The solvatochromism and other spectroscopic and photophysical characteristics of four azo disperse dyes, derived from 2-amino-5-nitrothiazole, were evaluated and interpreted with the aid of experimental data and quantum mechanical calculations. For the non-substituted compound two conformers, **E** and **Z**, were proposed for the isolated molecules, being the second one considerably less stable. The optimization of these structures in combination with a SCRF methodology (IEFPCM, simulating the molecules in a continuum dielectric with characteristics of methanol), suggests that the **Z** form is not stable in solution. This same behaviour is expected for the substituted compounds, which is corroborated by experimental data presented in previous investigations [A.E.H. Machado, L.M. Rodrigues, S. Gupta, A.M.F. Oliveira-Campos, A.M.S. Silva, J. Mol. Struct. 738 (2005) 239–245]. For the substituted compounds, two forms derived from **E** conformer (**A** and **B**) are possible. Quantum mechanical data suggest for the isolated molecules, that the low energy absorption band of the **E** conformers involve at least two close electronic states, having the low-lying excited state a $^1(n,\pi^*)$ nature, and being the S_2 state attributed to a $^1(\pi,\pi^*)$ transition. The data also suggest a small energy gap between the absorption peaks of **A** and **B**, related to the easy conversion between these forms. For the structures optimized in combination with the applied SCRF methodology, an states inversion is observed for the substituted compounds, with a considerable diminish of the energy gap between **A** and **B** absorption peaks. The electronic spectra of these compounds are quite sensitive to changes in the solvent polarity. The positive solvatochromism is more evident in aprotic solvents, probably due to the polarization induced by the solute. These compounds do not fluoresce at 298 K, but present a small but perceptible fluorescence at 77 K, which seems to be favoured by the nature of the group in the 2′-position of the phenyl ring. Moreover, such compounds present expressive values for first hyperpolarizability, which implies in good non-linear optics (NLO) responses and photoswitching capability.

1. Introduction

Progress in areas such as optical communication, optical computing, dynamic image processing, and data storage, would be greatly enhanced by the availability of materials with sufficiently large non-linear optics (NLO) responses combined with other desirable properties, such as photoswitching. In view of this, extensive research efforts have been directed towards the preparation of more efficient photon-manipulating materials [1–5].

It is known that organic molecules formed by a donor–acceptor pair connected to a π-delocalized framework present attractive NLO characteristics, which can be estimated from their hyperpolarizabilities [1,5,6]. The first hyperpolarizability, for example, gives information about the material capability to generate second order non-linear effects, such as: second harmonic generation, sum of frequency, parametric amplification and others [6].

Azo dyes are of particular interest since they can be readily prepared with a wide range of donor and acceptor groups. Besides, the

* Corresponding author. Tel.: +55 34 3239 4428; fax: +55 34 3239 4208.
E-mail address: aeduardo@ufu.br (A.E.H. Machado).

1010-6030/$ – see front matter © 2008 Elsevier B.V. All rights reserved.
doi:10.1016/j.jphotochem.2008.04.012

usually good planarity of the azo bridge which should contribute to larger π electron transmission effects [7–10]. In particular, azobenzenes, besides NLO properties, tend to exhibit photoswitching properties due to photo-induced *cis–trans* isomerization, making them promising for several technological applications [9].

Colour chemistry studies have demonstrated that the replacement of a benzene ring by a less aromatic heterocycle in typical donor–acceptor chromogens, such as azo and stilbene dyes, results in significant bathochromic shift of the visible absorption spectra [5,11,12], evidencing the enhancement of molecular hyperpolarizability [5]. Chippendale and co-workers described polymorphism for Disperse Red 278 due to slow exchange between two conformers [13]. Following the preparation of dyes **1**–**4** [14], a detailed investigation of dye **3**, by NMR, allowed us to assume that two forms were present (**A** and **B** conformers) in deuterochloroform solution and in the solid state, coexisting in equilibrium in an approximately 1:1 ratio at room temperature [15]. Besides, the polymorphism involving the *trans* form, *cis–trans* isomerization should also be considered. The understanding of how these phenomena correlate is one of the objectives of this paper.

In the present work, spectroscopic, photophysical and theoretical data were used to characterize the compound 2-(4′-*N*,*N*-diethylaminophenyldiazenyl)-5-nitrothiazole (compound **1**) and three acylamino derivatives of this dye (Fig. 1), and evaluate their solvatochromism and second order NLO capability. The synthesis and characterization of these compounds were previously reported [14].

2. Experimental

2.1. Spectroscopic measurements

UV/vis absorption, excitation and emission spectra were recorded using, respectively, a Shimadzu UV-2501 PC spectrophotometer and a HITACHI F-4500 spectrofluorimeter equipped with low temperature measurements accessories. The fluorescence spectra were obtained using the right angle configuration. For all experiments, the concentration of the solutions was between 2 and 3×10^{-6} mol dm^{-3}.

Fluorescence measurements were done at 298 and 77 K for solutions prepared in anhydrous ethanol. Fluorescence quantum yields were estimated from the corrected fluorescence spectra of the emission band with a maximum around 618 nm, using the secondary standard method. A methanol solution of cresyl violet ($\Phi_F = 0.54 \pm 0.03$; $\lambda_{exc} = 580$ nm) was used as fluorescence standard [16]. For these measurements, all solutions were prepared to present absorbance lower than 0.100 at the excitation wavelength to avoid light reabsorption effects. In the low temperature measurements, argon was used to deoxygenate the solutions. The xenon lamp was operated at 950 V, with the scanning rate adjusted at 240 nm min^{-1}. The emission and excitation slits were fixed at 2.5 mm.

All solvents (methanol, ethanol, 1-propanol, 2-propanol, 1-butanol, 2-butanol, 1-pentanol, 1-octanol, water, ethylene-glycol, *n*-hexane, chloroform, carbon tetrachloride, dimethylsulfoxide and acetone) were analytically pure or spectroscopic grade and were used as received.

2.2. Quantum chemical calculations

The molecular structure of these compounds was previously assessed using the PM3 semi-empirical method [17,18]. Afterwards, the optimization was refined using a Density Functional Theory (DFT) procedure based on the hybrid functional B3LYP, using the 6-31g(d,p) atomic basis set [19], from which the dipole moments and total energy of each system studied were estimated. These calculations were performed using the Gaussian 03W package [20,21]. The Berny analytical gradient was used in all DFT optimizations. The requested convergence limit on root mean square (RMS) density matrix was 1×10^{-8} and the threshold values for the maximum force and the maximum displacement were 0.000450 and 0.001800 a.u., respectively. Additionally, optimizations using a Self-Consistent Reaction Field (SCRF) methodology based on the IEFPCM (Integral Equation Formalism of Polarized Continuum Solvation Method) model [20] were done, defining methanol as solvent, to evaluate the influence of the solvent on the studied parameters. The 6-31g(d) atomic basis set was applied for this case.

The optimized structures (isolated molecules and the ones obtained by the application of the SCRF methodology) were used to estimate the components of the hyperpolarizability tensor [22], obtained by single point calculations using the PM3 semi-empirical method [18,23]. Application of these parameters in the following equation:

$$\langle\beta\rangle = [(\beta_{xxx} + \beta_{xyy} + \beta_{xzz})^2 + (\beta_{yyy} + \beta_{yzz} + \beta_{yxx})^2 + (\beta_{zzz} + \beta_{zxx} + \beta_{zyy})^2]^{1/2} \quad (1)$$

permitted to estimate the average value of the first hyperpolarizability, $\langle\beta\rangle$. The values of $\langle\beta\rangle$ are expressed in electrostatic units (1 a.u. = 8.6393×10^{-33} cm^5 esu^{-1}).

The excitation energies and oscillator strengths for the first 15 states of each of the studied compounds, were computed by TD-DFT calculations [24,25] using the 6-31g(d) atomic basis set. For the optimized structures based on the IEFPCM SCRF procedure, the TD-DFT calculations were done considering the structures previously optimized using the same SCRF methodology.

The state energies of the relaxed structures of compound **1** in the S_1 and S_2 states, optimized using the SCRF methodology combined with the Configuration Interaction Singles (CIS) approach [20] and the less expensive 3-21g* atomic basis set [26], were obtained by TD-DFT calculations based on the B3LYP hybrid functional and the 6-31G(d) atomic basis set. For these structures and for the S_0 state, the bond orders of some bonds were estimated using single point calculations based on the PM3 semi-empirical method [18].

Fig. 2 presents the **E**(**A**) conformation of compound **3**. The numbered atoms correspond to the geometric parameters used during the discussion. A representation of the **E**(**B**) conformation of this compound can be found in Ref. [15].

2.3. First hyperpolarizability measurements

The first hyperpolarizability ($\beta_{TOT} = \beta_{HRS}$) was measured using an extension of the conventional Hyper-Rayleigh Scattering technique (HRS) [27], named pulse trains hyper-Rayleigh Scattering (PTHRS). This technique allows improved and fast measurements, since mechanical movements, which could vary the intensity, are eliminated and higher frequency rates can be applied to acquire a large body of statistical data in a short time.

The samples were pumped by pulse trains composed by approximately 20 pulses of 70 ps separated by 13 ns, delivered by a Q-switched and mode-locked Nd:YAG laser at 1064 nm. As the complete Q-switch pulse train was used to pump the samples, each measurement involved more than ten different intensities of mode-lock pulses. To avoid noise and other than hyper-Rayleigh contributions (e.g. solvent ionization) the maximum intensity was left at the threshold of solution ionization, using for this purpose two crossed polarizers to limit the laser intensity. Moreover, any signal coming from another kind of process (e.g. two-photon fluorescence) would have to fall within the 3 ns response time of the

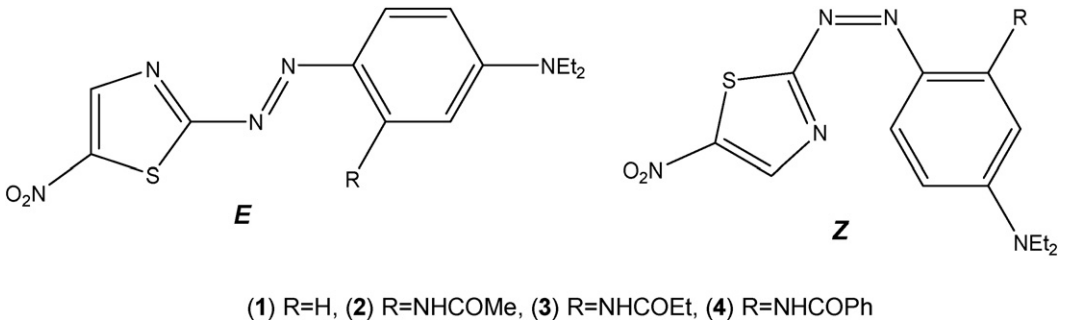

Fig. 1. Representation of the **E** and **Z** isomers of compounds **1**–**4**.

photomultiplier to pass unnoticed. A description of the relevant parts of the experimental setup has been presented in Ref. [28].

At least six different concentrations were measured for each compound, including the pure solvent (ethanol). All samples were previously filtered using 0.22 μm Millipore filters, to eliminate impurities, capable to generate spurious signals. To account for signal losses due to the cuvette optical path, in case the compounds have strong absorption at the second harmonic frequency, the signals were corrected using a similar procedure to the one described by Clays et al. [29]. In essence, the signal is multiplied by a $10^{A/b}$ factor, in which A is the absorbance at 532 nm and b is the optical path of the sample.

3. Results and discussion

3.1. Spectroscopic measurements

Fig. 3 presents the absorption spectra of the studied compounds in methanol covering the 250–800 nm spectral range. A set of three bands is observed, being the low absorption band located in the 450–700 nm spectral interval. Fig. 3 inset presents the excitation spectrum of compound **1**, estimated simulating a continuum dielectric possessing characteristics of methanol by the use of the IEFPCM method. This spectrum furnishes a good approach of the experimental absorption spectrum. The peak absorption predicted as occurring at 523 nm is about 10% lower than the experimental value. The association of discrete solvent molecules and SCRF methodologies (results not shown) tends to reduce this difference. The theoretical spectrum also suggests that the absorption band in this spectral range involves a set of adjacent singlet–singlet transitions.

Despite the theoretical evidences that points the existence of another conformer, named **Z** (*cis*) conformer (Fig. 1) for the isolated compounds, and the photoswitching capability expected for these molecules, as observed for substituted azobenzenes [9,30], the calculus simulating the compounds in solution, suggest that this form must be an unsettled intermediate. Experimental results obtained for compound **3**, suggest the existence of only two con-

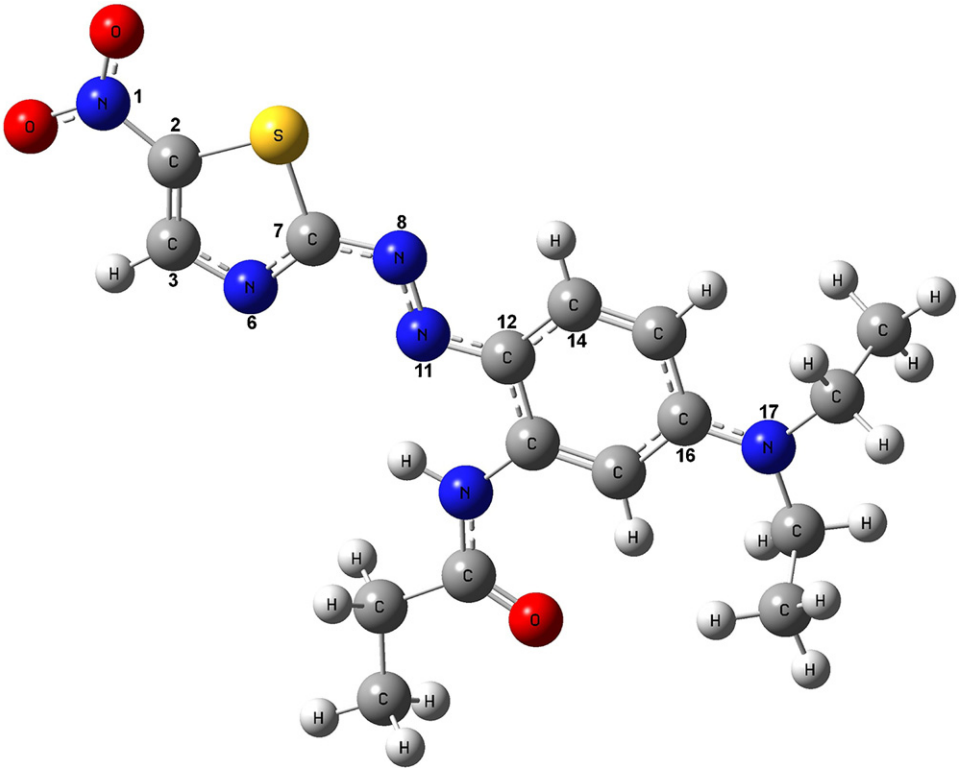

Fig. 2. Optimized structure for the **E(A)** conformer of compound **3**. The numbered atoms correspond to the geometric parameters used in the discussion.

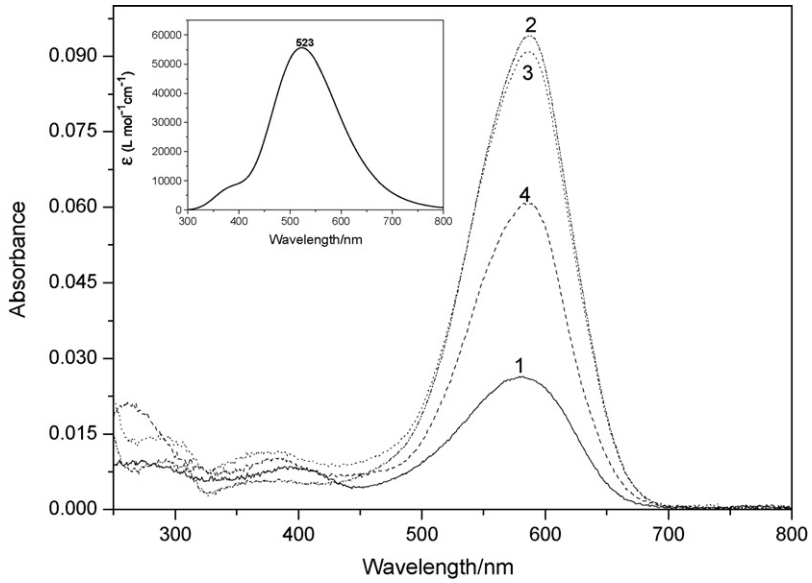

Fig. 3. Experimental absorption spectrum of compounds **1**–**4** in methanol. The concentration of the solutions ranged between 2.5 and 3.0×10^{-6} mol dm^{-3}. *Inset*: theoretical excitation spectrum of compound **1** in methanol, estimated by TD-DFT using a SCRF (IEFPCM) methodology.

Table 1
Electronic transitions, energy gaps, excitation wavelengths and oscillator strengths (*f*), estimated for the studied compounds, isolated and solvated

Compound	Relative total energy[a] (kJ mol^{-1})	Electronic transition	$\Delta E(S_2,S_1)$ (eV)	ΔE(**B**,**A**) (eV)[b]	λ_{exc} (nm) (*f*)	λ_{max}^{exp} (nm)[c]
1,E	0.00	$S_0 \rightarrow S_1$ (n,π^*)	0.368	–	534 (0.000)	
		$S_0 \rightarrow S_2$ (π,π^*)	–	–	461 (1.102)	
1,E$_{solv}$[d]	−56.66	$S_0 \rightarrow S_1$ (n,π^*)	0.027	–	529 (0.001)	
		$S_0 \rightarrow S_2$ (π,π^*)	–	–	523 (1.370)	581
1,Z[e]	+57.70	$S_0 \rightarrow S_1$ (π,π^*)	0.730	–	588 (0.232)	
		$S_0 \rightarrow S_2$ (π,π^*)	–	–	437 (0.193)	
2,A	0.00	$S_0 \rightarrow S_1$ (n,π^*)	0.179	–	503 (0.000)	
		$S_0 \rightarrow S_2$ (π,π^*)	–	–	469 (1.201)	
2,A$_{solv}$[d]	−53.72	$S_0 \rightarrow S_1$ (π,π^*)	0.066	–	521 (1.429)	587
		$S_0 \rightarrow S_2$ (n,π^*)	–	–	507 (0.000)	
2,B	4.25	$S_0 \rightarrow S_1$ (n,π^*)	0.225	–	498 (0.000)	
		$S_0 \rightarrow S_2$ (π,π^*)	–	0.072	457 (1.150)	
2,B$_{solv}$[d]	−53.21	$S_0 \rightarrow S_1$ (π,π^*)	0.040	0.067	507 (1.370)	
		$S_0 \rightarrow S_2$ (n,π^*)	–	–	498 (0.001)	
3,A	0.00	$S_0 \rightarrow S_1$ (n,π^*)	0.177	–	503 (0.000)	
		$S_0 \rightarrow S_2$ (π,π^*)	–	–	469 (1.194)	
3,A$_{solv}$[d]	−54.27	$S_0 \rightarrow S_1$ (π,π^*)	0.066	–	521 (1.422)	587
		$S_0 \rightarrow S_2$ (n,π^*)	–	–	507 (0.002)	
3,B	4.27	$S_0 \rightarrow S_1$ (n,π^*)	0.223	–	498 (0.000)	
		$S_0 \rightarrow S_2$ (π,π^*)	–	0.072	457 (1.138)	
3,B$_{solv}$[d]	−53.09	$S_0 \rightarrow S_1$ (π,π^*)	0.037	0.067	507 (1.362)	
		$S_0 \rightarrow S_2$ (n,π^*)	–	–	499 (0.000)	
4,A	0.00	$S_0 \rightarrow S_1$ (n,π^*)	0.150	–	502 (0.005)	
		$S_0 \rightarrow S_2$ (π,π^*)	–	–	474 (1.079)	
4,A$_{solv}$[d]	−59.35	$S_0 \rightarrow S_1$ (π,π^*)	0.075	–	523 (1.348)	584
		$S_0 \rightarrow S_2$ (π,π^*)	–	–	507 (0.010)	
4,B	5.78	$S_0 \rightarrow S_1$ (n,π^*)	0.192	–	498 (0.000)	
		$S_0 \rightarrow S_2$ (π,π^*)	–	0.062	463 (0.990)	
4,B$_{solv}$[d]	−59.75	$S_0 \rightarrow S_1$ (π,π^*)	0.055	0.058	510 (1.248)	
		$S_0 \rightarrow S_2$ (π,π^*)	–	–	499 (0.010)	

[a] Based on the total energy, *E*(RB + HF − LYP), for each conformer.
[b] Energy difference between the most intense excitation peaks related to A and B conformers.
[c] Data for solutions prepared in methanol.
[d] For **2,Z**, **3,Z** and **4,Z**, the values are, respectively, 61.15, 61.17 and 62.88 kJ mol^{-1}.
[e] Including two CH_3OH molecules, one interacting with the diethylamino group and the other with the nitro group, in a calculation based on the IEFPCM model.

formers for this compound, related to the **E** form [15]. However, based on theoretical studies of the **E** and **Z** conformers of compound **1**, the occurrence of a *cis–trans* photoisomeration was considered for the isolated compounds, or in the gas phase. The *trans* (**E**) form is energetically the favoured one. For example, the relative difference between the total energies related to the ground state of **1,Z** and **1,E** is about 57.70 kJ mol^{-1} (Table 1). Systematically, the relative energy difference between **Z** and **E** forms for the substituted compounds assumes value higher than 60 kJ mol^{-1} (see Supplementary Data). The optimization of these compounds in combination with the IEF-PCM method suggests that the **Z** form is not a stable conformer.

For all conformers, the theoretical data suggest that the most intense absorption peak of each form involves predominantly *HOMO* and *LUMO* orbitals (not shown). For the isolated compounds the low-lying state corresponds to a $^1(n,\pi^*)$ transition. A second, "fully allowed" $^1(\pi,\pi^*)$ $S_0 \rightarrow S_2$ transition is responsible for the most intense absorption peak. In Fig. 3 inset the most intense absorption peak corresponds to the $S_0 \rightarrow S_2$ $^1(\pi,\pi^*)$ electronic transition for compound **1**. For the other compounds in solution, the most intense absorption peak corresponds to the $S_0 \rightarrow S_1$ $^1(\pi,\pi^*)$ transition, the result of a state inversion. For compound **4**, the first and second transitions change to a $^1(\pi,\pi^*)$ character for the solvated specie, probably due to the participation of the substituent group in the 2′-position of the phenyl ring, in the electronic conjugation. This state inversion is most probably a direct consequence of the solute–solvent interactions, which affect the energy gap between S_2 and S_1, $\Delta E(S_2,S_1)$, reducing it (Table 1). These solute-solvent interactions suggest an increase in charge transfer between the diethylamino moiety and the rest of the molecule, mainly favoured by strong polar solute–solvent interactions [31]. It is known that the combination of electron-donor, electron withdrawing groups and solvation effects, especially when involving strong polar solute–solvent interactions, like hydrogen bonding, intensifies electron delocalization, with positive implications on the photophysical and spectroscopic properties and consequently on the NLO properties of these compounds.

The occurrence of state inversion due to solute-solvent interactions, when neighbour states are sufficiently close to each other, has been considered by many researchers [31–33]. Seixas de Melo et al. [33] reported, based on photophysics studies of coumarins, that, for this class of compounds, the S_1 state is typically $^1(n,\pi^*)$ and that the potential energy surfaces corresponding to the S_1 and S_2 states are close. Substitutions or changes in the solvent polarity may reduce the energy gap between these states, promoting the mixing or inversion, which can result in an S_1 (π,π^*) state. The curtailment of the bond between the diethylamino group and the aromatic ring, observed between the structures in the S_0 and S_1 states has been evidenced in a previous work as being due to the electronic coupling between the diethylamino group and the π system of the rest of the molecule during electronic excitation [31].

As the solute–solvent interactions become more intense, internal conversion (IC), due to the increase in the vibronic coupling, tends to be increasingly important as deactivation route of the excited state [31,32,34,35]. An implication of this behaviour is the almost imperceptible fluorescence presented by these compounds.

Between the **A** and **B** conformers, a small energy gap is expected for the most intense transition (Table 1), which diminishes significantly in the excitation spectra calculated using a SCRF methodology. These small values suggest the conversion between these forms requires very low energy amounts to occur. Previously [15], using a semi-empirical method (PM3), we estimated an energy barrier of about 706 cm^{-1} for the **B** → **A** conversion of compound **3**. In this work, the estimated energy gap using TD-DFT for this same compound corresponds to an energy barrier of about 582 cm^{-1} for the isolated specie. In solution, the estimated energy gap reduces to about 0.067 eV (543 cm^{-1}).

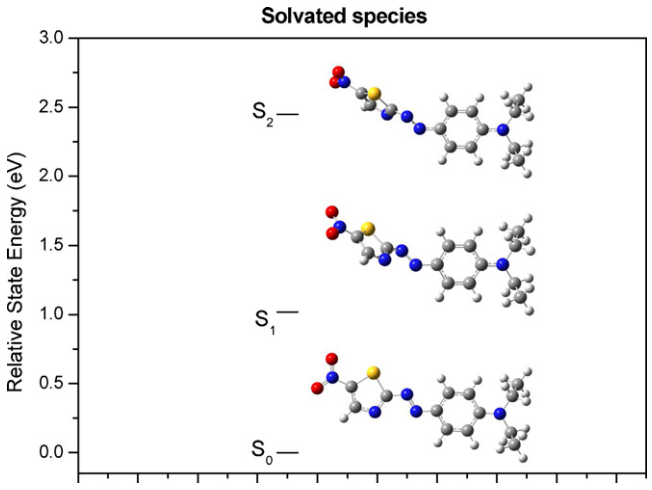

Fig. 4. Energy diagram for the S_0 state and the relaxed S_1 and S_2 structures of compound **1**, calculated using a SCRF methodology. The S_1 and S_2 structures were previously optimized using the CIS approach. In the S_1 state, the dihedral angle between the 4′-*N*,*N*-diethylaminophenyl and the 5-nitrothiazole groups is about +55.906°. For S_2, this dihedral angle is −56.817°, whereas for S_0 is about −0.109°.

Unlike to typical azobenzenes [30], the energy gap between the low-lying and the adjacent state, $\Delta E(S_2,S_1)$ seems to be small. For compound **1** the estimated energy gap is approximately 0.37 eV (35.59 kJ mol^{-1}). This energy gap tends to suffer a drastic decrease when solvent models are introduced in the calculation. For this same compound, optimized using a SCRF approach, this energy gap is 0.03 eV (2.89 kJ mol^{-1}).

For the substituted dyes, the moiety in the 2′-position of the aromatic ring seems to influence the $\Delta E(S_2,S_1)$ value, decreasing it for the **E**(**A** and **B**) forms, probably caused by an increase in the electronic conjugation by the combination between the electron donor–acceptor character, more evident for planar compounds (lower differences for the compounds in the **E** form—ICT complexes), and the electron donor effect of the alkyl (inductive) and phenyl (inductive and mesomeric) groups. These values are systematically lower than the estimated for the isolated compound **1**, but they are not that much lower when solvent models are introduced in the calculation (Table 1).

An energy diagram of the S_0, S_1 and S_2 states of compound **1** correlated to the corresponding structures is presented in Fig. 4 and Table 2. It was built based on the state energies (in eV) of the relaxed and solvated structures.

The structure that corresponds to the solvated and relaxed S_1 state of compound **1** differs in some aspects from the S_0 state. As shows Table 2, this implies in changes in the N(6)C(7)N(8)N(11) and N(8)N(11)C(12)C(14) dihedral angles, the first from −0.106° to +0.605°, and the second from 0.000° to +23.729°, due to a decrease in the bond order of the bond N(11)C(12) probably caused by the lack of structural symmetry. This partial loss of planarity, results in changes in the electronic conjugation and properties as the dipole moment, which suffers an increase of about 13%, and $\langle\beta\rangle$, whose calculated value for the specie in the S_1 state increased 28% in comparison with the value calculated for S_0 (Table 3). It is known from empirical observations that the second order response of NLO properties can be enhanced increasing the electronic asymmetry (compounds need to be non-centrosymmetric in order to present large β responses) or the conjugation length between the substituents [1,6]. Efficient second order NLO properties are usually related to compounds where an intramolecular

Table 2
Some relevant geometric parameters (see Fig. 2 for the atom numbering) and bond orders estimated for compound **1** in the S_0, S_1 and S_2 states, optimized using a SCRF (IEFPCM, simulating methanol as solvent) methodology

Parameter	Conformer (*E*)					
	S_0		S_1		S_2	
		B.O.		B.O.		B.O.
Bond length (Å)						
$d_{N(1)C(2)}$	1.410	0.96	1.383	0.99	1.383	0.99
$d_{C(2)C(3)}$	1.382	1.47	1.355	1.48	1.355	1.48
$d_{C(3)N(6)}$	1.349	1.34	1.357	1.33	1.357	1.33
$d_{N(6)C(7)}$	1.332	1.48	1.320	1.46	1.320	1.46
$d_{C(7)N(8)}$	1.368	1.12	1.348	1.15	1.348	1.15
$d_{N(8)N(11)}$	1.297	1.65	1.272	1.67	1.272	1.67
$d_{N(11)C(12)}$	1.365	1.18	1.374	1.15	1.374	1.15
$d_{C(12)C(14)}$	1.424	1.26	1.397	1.29	1.397	1.29
$d_{C(16)N(17)}$	1.357	1.24	1.360	1.21	1.360	1.21
Dihedral angle (°)						
$\gamma_{C(14)C(12)N(11)N(8)}$	0.000	–	23.729	–	−24.384	–
$\gamma_{C(12)N(11)N(8)C(7)}$	−179.98	–	−131.80	–	131.93	–
$\gamma_{N(11)N(8)C(7)N(6)}$	−0.106	–	0.605	–	−0.719	–

charge transfer (ICT) process occurs. The ICT processes are usually one-dimensional in character, being associated to appreciable dipole moment changes, $\Delta\mu$, between the ground and the first excited state, currently identified as the "charge transfer state" [1,36], related to the electron transfer between the ground and excited state. Typical compounds showing this kind of properties are π-conjugated molecules with a **D**-π-**A** structure, where **D** and **A** are, respectively, electron donor and acceptor groups, and π is a π-conjugated system. This push–pull characteristic generally leads to high β values, which can be further maximized through an adequate substitution of electron **D** and **A** groups. It is known that chromophores possessing the largest β responses contain donor and acceptor substituents linked by a π-electron bridge [1], and that the nature of these groups exerts an important role in the intensification of the NLO properties of organic compounds [1,37].

The relaxed S_1 and S_2 states of the studied compounds present oscillator strengths compatible with π,π* transitions (e.g. for compound **1** the oscillator strength is about 0.129 for the solvated molecule in the S_1 state, and 0.583 in the S_2, whereas the estimated for the isolated molecule in the S_1 is 0.056), corroborating the studied compounds do not fluoresce at 298 K, presenting very low Φ_F values at 77 K.

As observed for compound **1**, the formation of the S_1 state of the other compounds also results in loss of structural symmetry attributed to the torsion between the azo and 5-nitrothiazole groups and the 4′-*N*,*N*-diethylaminophenyl one, due to the rotation of the N(11)–C(12) bond and increase in the charge transfer along the molecule (not shown). For S_2, similar behaviour is also observed.

3.2. Fluorescence measurements

These compounds do not show measurable fluorescence at 298 K, but present weak fluorescence at 77 K. Strong energy dissipation from S_1 by non-radiative processes due to the occurrence of solute–solvent interactions favours the increase in the vibronic coupling, with profound implications on the deactivation of the excited state. Fig. 5 presents the emission spectra obtained for these dyes, and two excitation spectra related to compounds **1** and **3**.

For the substituted dyes two bands are observed (Fig. 5a), the more intense at 612 nm and a shoulder-like one of very low intensity, near 660 nm. Compound **1** presents a practically imperceptible fluorescence signal (Fig. 5b), with an emission band with peak value at 651 nm which should be equivalent to the peak at about 660 nm, observed for the substituted dyes. The similarities between these emission spectra leads us to consider that the band centred at 660 nm is related to the **A** conformers, structurally equivalent to compound **1**. Hence, the most intense signal around 612 nm should be related to the **B** conformers. Due to the occurrence of intramolecular hydrogen bonding, these species must present lower mobility at 77 K, relative to the **A** conformers, which explains the difference between the Φ_F values presented by the substituted compounds and compound **1** (Fig. 5c). After exhaustive measurements under low temperature, no fluorescence evidence was found of the **Z** form. Synchronous spectra of these compounds (see Supplementary Data) confirm the existence of only two emissive species for the substituted compounds and one for compound **1**.

Fig. 5c presents the ratio between the estimated Φ_F and the nature of the amide moiety. A trend to increase Φ_F is observed as the size of the R group increases (compounds **1**–**3**), most probably due to the increase of the energy barrier for **A** ↔ **B** conversions. The small fluorescence quantum yield values (Φ_F) calculated from the emission band centred at 615 nm and the fact phosphorescence is not detected indeed at 77 K, confirm that internal conversion, related to structure mobility and solute–solvent interactions, is the

Table 3
Average value of the first hyperpolarizability, dipole moment (μ) and its components, calculated for isolated and solvated compounds

Dye	$\langle\beta\rangle \times 10^{30}$ (cm^5 esu^{-1})	μ (Debye)	μ_x	μ_y	μ_z
1,E	168.42	12.7053	12.7012	0.3242	0.0413
1,E$_{solv}$[a]	193.10	19.9921	19.9871	0.4436	0.0519
1,E$_{solv}$ (S_1)$_{relaxed}$[a]	247.30	22.5662	22.5579	0.3426	0.5069
1,Z	89.65	10.9773	−10.8143	1.8741	−0.2004
2,A	175.05	10.4553	−10.4078	−0.9951	0.0166
2,A$_{solv}$[a]	170,80	16.4319	−16.3392	−1.7415	0.0865
2,B	158.76	10.8216	−10.7854	−0.8674	0.1719
2,B$_{solv}$[a]	148.74	16.5379	−16.4639	−1.5391	0.2695
3,A	174.16	10.5562	−10.4931	−1.1524	−0.0041
3,A$_{solv}$[a]	168.31	16.5684	−16.4534	−1.9482	0.0410
3,B	157.64	10.8867	−10.8613	−0.7415	0.0425
3,B$_{solv}$[a]	146.96	16.5806	−16.5266	−1.3342	0.0968
4,A	166.70	10.2182	−10.2114	−0.3725	−0.0172
4,A$_{solv}$[a]	163.25	15.8272	−15.8153	−0.5314	0.3047
4,B	151.11	10.4194	10.3898	0.7198	0.3112
4,B$_{solv}$[a]	142.68	15.8599	15.8253	0.8391	0.6273
Der 1	269.40	12.9363	12.8918	1.0580	0.1739
Der 2	444.96	14.4426	14.3047	1.9719	0.2734

[a] $\langle\beta\rangle$ estimated using the optimized in combination with the IEFPCM model, simulating methanol as solvent.

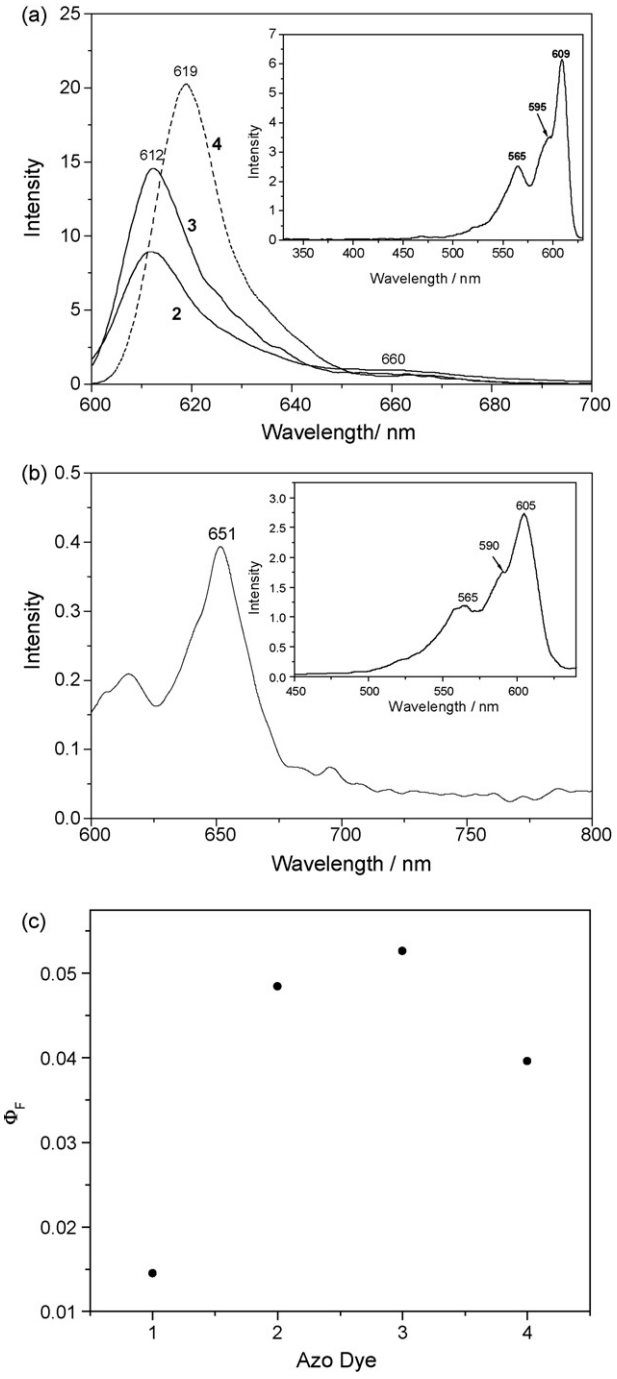

Fig. 5. Fluorescence and excitation spectra at 77 K: (a) fluorescence spectra of compounds **2**–**4**, and excitation spectrum of compound **3** (λ_{em} = 640 nm); (b) emission (λ_{exc} = 593 nm) and excitation (λ_{em} = 650 nm) spectra of compound **1**; (c) Φ_F as function of the dye.

preferential route for the excited state deactivation of these compounds [39,41]. This agrees with the values estimated for Φ_{IC} in ethanol at 77 K (around 0.99 for the non-substituted compound and 0.96 for the other three compounds), when the molecular mobility can be significantly reduced. The solute–solvent interactions, mainly hydrogen bonds involving the diethylamino moiety, result in the increase of the vibronic coupling [31,32,38,40,41] which tends to suppress the fluorescence of such compounds by internal conversion, due to the increase in the density of states of such solute–solvent complexes. The fluorescence intensity of compound **4** does not follow that pattern possibly due to the non-planarity of the phenyl ring.

In a previous paper [15], the coexistence between the **A** and **B** forms of compound **3** was evidenced by experimental and theoretical data. NMR data show that at room temperature they coexist in a 1:1 ratio but at 218 K the **A** form is slightly favoured (55:45), in agreement with results from theoretical calculation (60:40). So, no experimental nor theoretical evidence support the existence of the **Z** form as a stable specie in solution. This is also supported by the several unsuccessful tentative to optimize this form using a continuum dielectric (SCRF) model or considering the association of this procedure with discrete solvent molecules. In fact, a comparison of the total energy for each set of studied forms show the **Z** form is considerably less stable than the other conformers. An other aspect that is worth mentioning is that the species optimized using the SCRF methodology tend to be more stabilized than the isolated ones, and that the **A** form is systematically the most stable.

A thermodynamic treatment of the theoretical data [15] has suggested that the **B** form is less stable than the **A** one. Our results based on the analysis of the DFT and TD-DFT data agree with this. An additional stabilization for these conformers due to solvation effects was also observed when these molecules were optimized combined with certain discrete molecules. The ΔG_r° estimated for **A** → **B** conversion under this condition was attributed to solute–solvent interactions, mainly intermolecular hydrogen bonding. In methanol and chloroform the energy barrier is significantly lower than the calculated for the isolated form. Differently, for **B** combined with DMSO, the value is 41% higher, indicating the formation of intramolecular hydrogen bonding benefits this form in this situation.

3.3. Solvatochromic shifts

The experimentally observed solvatochromic shifts for compound **2** in protic and aprotic solvents are shown in Fig. 6, based on the dependence between the absorption peak corresponding to the $S_0 \rightarrow S_1\ ^1(\pi,\pi^*)$ (Table 1) electronic transition for this compound in the **E** form and the $E_T(30)$ scale [42]. This behaviour is very similar for the other compounds.

The observed bathochromic shift can be explained by assuming polar interactions between these compounds in the excited state and the solvent occur with the formation of charge transfer complexes (electron donor–acceptor (EDA) complexes). This is in agreement with the shape of these absorption bands and the sensitivity of λ_{max} on the solvent polarity [40]. For non-polar solvents, the cause of the bathochromic shift may be the strong polarization induced by these dyes, which present significant values of dipole moment (Table 3) and polarizability (not shown).

Fig. 7 presents the plot between λ_{max}(abs) and the empirical parameter $E_T(30)$ [42] for compounds **1** (Fig. 7, inset) and **2**.

The good sensitivity of these compounds to solvent polarity should be directly related to the small energy gap between S_1 and S_2 and the nature of these states [31,33]. The observed decrease in the molar absorptivity as solvent polarity increases must be related to the increasing mixture of states [38,40,41]. The observed small changes in λ_{max} observed for protic solvents should be associated with small variance in the stability of the EDA complex as polarity of such solvents varies, explaining the very small changes in the energy gap between S_1 and S_2. Particularly for protic solvents the occurrence of hydrogen bonding must be responsible for the stability of such complexes. Water and ethylene glycol (Fig. 7, points 14 and 15), able to form more than one hydrogen bond, do not follow the observed tendency.

A direct relationship between the molar absorptivity and solvent polarity is an important behaviour, very evident in protic

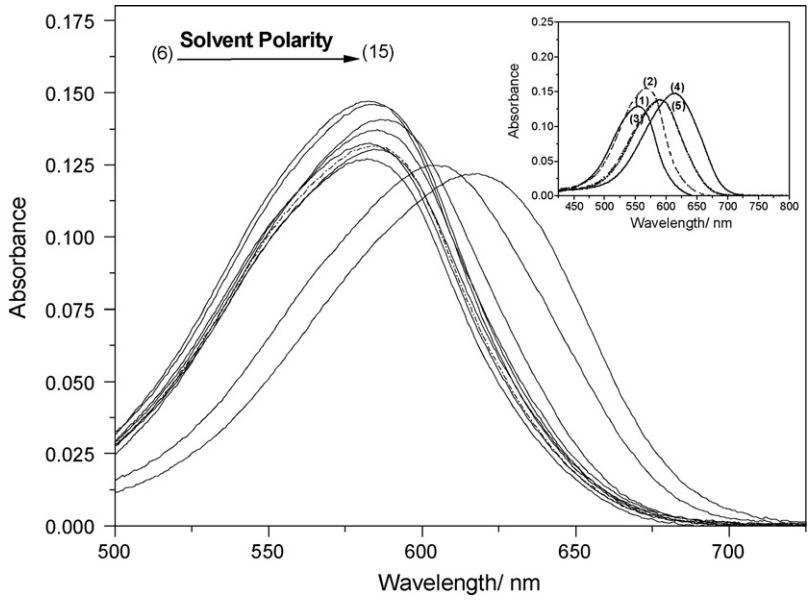

Fig. 6. Solvatochromic shifts for compound **2**, in protic and aprotic (inset) solvents: *n*-hexane (1), carbon tetrachloride (2), chloroform (3), acetone (4), dimethylsulfoxide (5), 2-butanol (6), 1-octanol (7), 2-propanol (8), 1-pentanol (9), 1-butanol (10), 1-propanol (11), ethanol (12), methanol (13), ethylene glycol (14), water (15).

solvents (excluding water and ethylene-glycol). This is an suggests the solute–solvent interactions, mainly the strongly polar ones, such as the hydrogen bonds, tend to favour electronic delocalization and consequently the intramolecular charge transfer in such compounds. An implication of this is the intensification of the NLO properties.

Hutchings et al. [11] observed that plots of the transition energies against single-parameter descriptors of solvent polarity, such as the $E_T(30)$ scale [42], are unsatisfactory to describe the solvatochromism of arylazo and heteroarylazo compounds based on *N*,*N*-diethyl-*m*-acetylaminoaniline and *N*,*N*-diethyl-*m*-toluidine, suggesting the use of multiparameter scales, such as the Kamlet–Taft plot. However, the $E_T(30)$ scale describes in an adequate manner the solvatochromic behaviour of the dyes studied in this work.

The observation of a bathochromic shift as solvent polarity raises suggests that the molecular hyperpolarizability of such compounds tends to increase with the strength and specificity of the solute-solvent interactions [5,11,12].

3.4. Dipole moments and first hyperpolarizability

The compounds under study present considerable planarity in the ground state, suggesting good π-electron delocalization

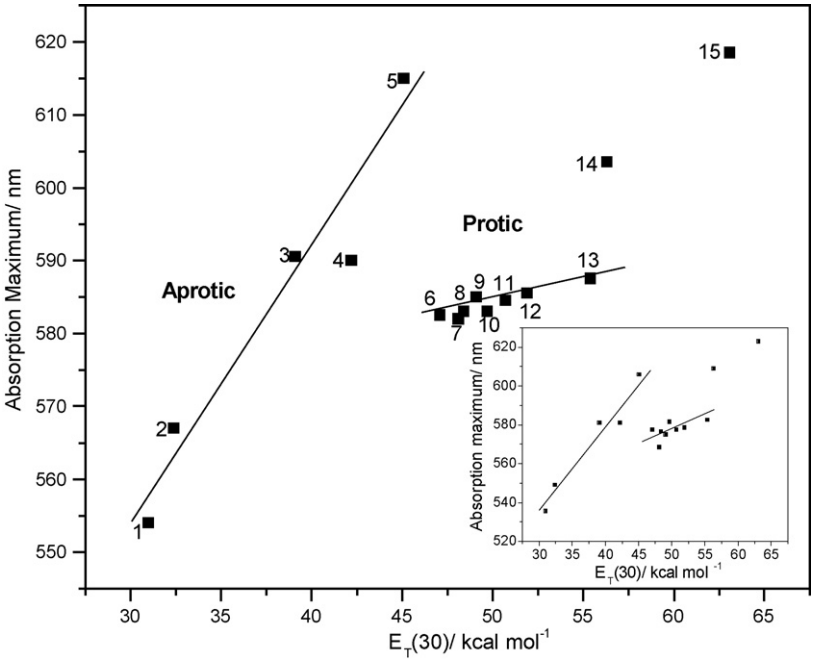

Fig. 7. Plot of λ_{max} (abs) vs. $E_T(30)$ for compound **2** in different solvents: *n*-hexane (1), carbon tetrachloride (2), chloroform (3), acetone (4), dimethylsulfoxide (5), 2-butanol (6), 1-octanol (7), 2-propanol (8), 1-pentanol (9), 1-butanol (10), 1-propanol (11), ethanol (12), methanol (13), ethylene glycol (14), water (15). *Inset*: plot of λ_{max} (abs) vs. $E_T(30)$ for compound **1**.

Table 4
First hyperpolarizability data measured by HRS in ethanol for the studied compounds compared with the $\langle\beta\rangle$ values (see Eq. (2))

Compound	β_{HRS} (cm^5 esu^{-1})	$\langle\beta\rangle$ (cm^5 esu^{-1})
1	1724×10^{-30}	193×10^{-30}
2	1030×10^{-30}	160×10^{-30}
3	1563×10^{-30}	158×10^{-30}
4	657×10^{-30}	152×10^{-30}

due to the ability to perform intramolecular charge transfer [7,31,32,43], acting as push–pull compounds. The electron density mapped with ESP (not shown) indicate positive charge density over the diethylamino group and a negative density distributed between the nitrogen from thiazolyl, azo and the oxygen atoms from the nitro group, the highest negative density being centered on the later, suggesting a charge transmission across the molecule. For the substituted compounds, the negative charge density also involves the lateral group at the 2′ position of the phenyl ring. For the species optimized in combination with a SCRF methodology (IEFPCM), the electron delocalization is much more pronounced corroborating with the discussion presented in Section 3.1.

The electronic structure of the low-lying excited states suggests the possibility of technological application of such compounds, since it is known that the lowest-lying charge-transfer excited states of closed-shell systems are generally the responsible for the second-order non-linearities [1]. The average values of first hyperpolarizability, $\langle\beta\rangle$, for such compounds (see Table 3) suggest the experimental data might present very expressive values, which is confirmed by the data from HRS measurements (Table 4).

As suggest the data in Table 3, the use of a SCRF methodology to describe solute–solvent interactions shows a significant increase in the dipole moment, with the systematic increase of the μ_x component value, as well as in the components of the octapole moment (see Supplementary Data), which reflects positively in the estimated value for $\langle\beta\rangle$. This show the most effective interactions must occur on nitro and diethylamino groups. Despite these positive results, the continuum dielectric models are not capable to consider specific interactions between solute and solvent. In view of this, simulations were done using the combination of IEFPCM and the interaction between compound **1** and discrete molecules of methanol (unpublished results).

Expressive increases in the dipole moment, mainly the μ_x component, were estimated for the species optimized in combination with IEFPCM, or by the combination between the inclusion of discrete solvent molecules performing hydrogen bonding with the diethylamino and nitro groups, with positive consequences on the estimative of $\langle\beta\rangle$ and other electronic properties (unpublished results). In all situations, S_0 remains with a planar geometry, whereas S_1 presents a expressive torsion between the 4′-*N*,*N*-diethylaminophenyl and the 5-nitrothiazole groups.

The preference to apply the semi-empirical calculation to estimate $\langle\beta\rangle$ and other NLO parameters, is based on the fact that certain semi-empirical methods have been adequately parametrized to describe NLO properties [37,44,45]. The use of more accurate theoretical descriptions for the studied compounds tend to improve the estimated value for $\langle\beta\rangle$, approximating the theoretical values to the experimental ones. Otherwise, simulations exclusively based on *ab initio* and DFT methods are, in principle, capable to furnish better results. However, this requires more expensive computation time, each more complex and elaborated calculation, involving flexible, large and rich in diffuse functions basis sets and a suitable description of the environmental conditions surrounding the molecules [1,25,46,47].

All these compounds present expressive values of dipole moment, with a large contribution of the *x* component (Table 3). Due to the influence of the amide group at the 2' position of the phenyl ring, the resultant dipole moments for compounds **2**, **3** and **4** are lower than for compound **1**.

It is well known that non-linear optical properties of "push–pull" compounds can be improved extending the conjugation of the π-bridge and/or by modifications in the relative electron affinities of the donor and acceptor groups and in the dipole moment [9]. It has been reported that the first hyperpolarizability increases with the number of double bonds in a polyenic bridge [45]. A number of 10 conjugated double bonds have been suggested as a critical number for the saturation of this trend [45]. However, this "magic number" needs to be taken with care. Experimental studies involving cyanine dyes indicate that the maximum corresponds to only four double bonds, and that the limit number of double bonds is related to questions of conformational nature [48]. These considerations points indirectly to a problem: the synthesis of push–pull systems containing a substantial number of conjugated double bonds often tends to become difficult [49,50]. To evaluate this, the effect of the increase of the π-bridge including additional double bonds between the 5-nitrothiazolyl and the azo group on $\langle\beta\rangle$ was studied for two optimized compounds based on the structure of compound **1** (Fig. 8).

Based on the analysis of $\langle\beta\rangle$, an expressive increase in the average value of the first hyperpolarizability (Table 3) when compared to the value estimated for compound **1,E** was observed for these optimized structures. For **Der 1**, containing one C=C double bond the estimated increase in $\langle\beta\rangle$ was about 60%. For **Der 2**, containing three conjugated C=C double bonds, the increase compared to compound **1,E** was of 164%. An increase in the dipole moment could be observed. The observed effect is mainly related to μ_x, the higher magnitude component.

The size of the conjugated system is not the only variable to be adjusted aiming the increment in the NLO properties. As evaluated in this work, the kind of interactions between the electro-optic molecules and the solvent (or the surrounding medium) might be an important parameter for the development of organic-based electro-optic devices. Modifications in the relative electron affinity of the donor and acceptor groups or the substitution of the π bridge by mesoionic groups [45] can be interesting alternatives. Hence, the combination of these parameters should warrant significant values for the first hyperpolarizability of the class of compounds under study. For these compounds, the increase in the size of the π bridge has only a small influence on the dipole moment.

3.5. First hyperpolarizability measurements

To perform the HRS measurements the external reference method (ERM) [51] was employed, using *p*-nitroaniline (*p*-NA) in ethanol as standard, with β_{TOT} value for *p*-NA of 26.2 cm^5 esu^{-1} [52]. Typical quadratic HRS signals are shown in Fig. 9 for compound **4** in ethanol.

Fig. 9, inset presents the HRS signal as function of the molecular density for compound **4**, after the corrections previously mentioned were applied. The slope of each line is to be compared with the slope of the standard, as prescribed by the ERM [51].

The comparison between HRS experimental values ($\beta_{TOT} \equiv \beta_{HRS}$) and $\langle\beta\rangle$ estimated for each different conformation assumed for each of these compounds cannot be considered a trivial task. The experimental first hyperpolarizability should be probably the resultant of the first hyperpolarizabilities due to the different conformers assumed by these compounds in solution. It is possible that $\langle\beta\rangle$ that correlates with β_{TOT} involves the vector sum of $\langle\beta\rangle x_i$, in which $\langle\beta_i\rangle$ is the average value estimated for the

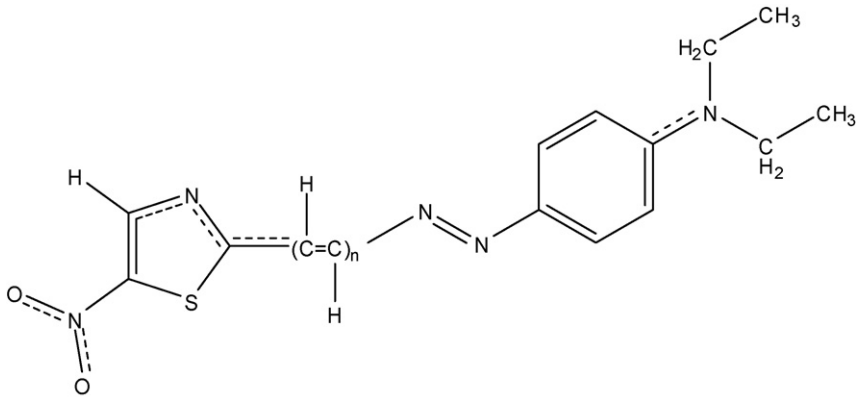

Fig. 8. Representation of the increase of a π-bridge between the 5-nitrothiazolyl and the azo groups for a structure based on dye **1,E**.

conformer *i*, and x_i is the corresponding molar fraction:

$$\beta_{TOT}\alpha\sum_i \langle\beta_i\rangle x_i \quad (2)$$

Considering the **A** and **B** forms are present in solution in an approximately 1:1 proportion, the $\langle\beta\rangle$ values estimated for the solvated species are presented in Table 4. Despite the quantitative discrepancy between $\langle\beta\rangle$ and β_{HRS} the same kind of behaviour is observed for compounds **1**, **2** and **3**. A somewhat different behaviour is presented by compound **4** in the comparison between $\langle\beta\rangle$ and β_{HRS}.

The compounds under study exhibit large signals, easy to detect, except for the high concentrations, in which the signal is strongly absorbed. Although all the measurements were performed with absorbance lower than unity to guarantee the validity of Lambert & Beer's law, some data deviated from the line. The experimental first hyperpolarizabilities are shown in Table 4, and compared with the $\langle\beta\rangle$ values (see Eq. (2)).

The discrepancies of value between theoretical and experimental data are well explained by a set of factors that were not completely considered in this manuscript. The prediction of quantitative NLO data for medium and large molecules using DFT, *ab initio* or even semi-empirical methods is still a methodological challenge [1]. The theoretical reproduction of experimental conditions to give quantitative data of NLO properties is a difficult, but not impossible, task.

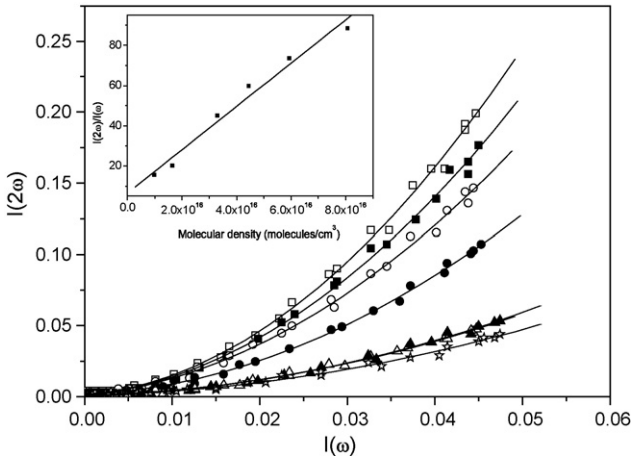

Fig. 9. HRS signals measured for solutions of compound **4** in ethanol, for six different molecular densities, as a function of the reference signal, in arbitrary units. The full lines are the corresponding quadratic fits. *Inset*: HRS signal as a function of molecular density of compound **4**. The straight line corresponds to the linear fit.

4. Conclusions

The analysis of the absorption spectra of the compounds under study with the aid of TD-DFT data discards the existence of the **Z** conformer in solution, as a stable conformer. The band in the 450–700 nm spectral interval is related to the **E** conformer, being, for the substituted dyes, the superposition of the absorption peaks corresponding to the **A** and **B** forms, very close in energy, principally for the solvated species. The quantum mechanical data suggest that the absorption band of the **E** conformers involve at least two closely related electronic states, being, for the isolated molecule, the low-lying excited state attributed to a $^1(n,\pi^*)$ transition, whereas the adjacent state is related to a $^1(\pi,\pi^*)$ one. The theoretical data suggests a state inversion for the substituted compounds in solution, most probably a direct consequence of the solute–solvent interactions. The occurrence of internal charge transfer in such compounds is directly influenced by these interactions, with very positive implications on NLO properties. The partial lack of planarity for these molecules in the excited state results in changes in the electronic conjugation, and appreciable dipole moment increment.

The forms **A** and **B** are sensitive to changes in solvent polarity, presenting positive solvatochromism, which is more pronounced in aprotic solvents, probably due to the formation of solute–solvent complexes. For protic solvents, as only small variations in the strength of the solute–solvent interactions must occur as increases solvent polarity, small bathochromic shifts are observed. These compounds do not fluoresce at 298 K, deactivating the excited state mainly by internal conversion, influenced principally by formation of solute–solvent complexes, and to a minor extent by their internal mobility. At 77 K they tend to present a small but perceptible fluorescence whose quantum yield is affected by the nature of the group at the 2′-position of the phenyl ring. The fluorescence band at about 612 nm corresponds to the emission of the **B** form. The band centered at about 660 nm was attributed to the **A** form.

The expressive values for the first hyperpolarizability estimated for these compounds and confirmed by HRS measurements, suggest they are good candidates for photonic technological applications. Despite the quantitative discrepancy between $\langle\beta\rangle$ and β_{HRS}, a similar behaviour is observed for compounds **1**, **2** and **3**.

Despite the observed limitations to express systems like the studied ones, the use of a combination of DFT and semi-empirical methodologies showed to be able to furnish complimentary information about the behaviour of these systems.

Acknowledgments

We thank to the Universidade do Minho and FCT-Portugal (POCTI-SFA-3-686) for financial support and Ahmadu Bello University, Zaaria, Nigeria, for a sabbatical leave of P. Nkeonye. Radim Hrdina thanks VZ MSM 0021627501 for financial support. The Brazilian researchers thank the FAPEMIG (PRONEX), CNPq and CAPES for financial support and research grants. AEHM is particularly indebted to Professor Julien F.C. Boodts for the revision of the English language and valuable suggestions, and to Drs. Divinomar Severino and Valdemir Velani for the technical support in some fluorescence measurements.

Appendix A. Supplementary data

Supplementary data associated with this article can be found, in the online version, at doi:10.1016/j.jphotochem.2008.04.012.

References

[1] D.R. Kanis, M.A. Ratner, T.J. Marks, Chem. Rev. 94 (1994) 195–242.
[2] D.J. Williams, Thin Solid Films 216 (1992) 117–122.
[3] P.J. Mendes, J.P. Prates Ramalho, A.J.E. Candeias, M.P. Robalo, M.H. Garcia, J. Mol. Struct. (Theochem.) 729 (2005) 109–113.
[4] N.M.F.S.A. Cerqueira, A.M.F. Oliveira-Campos, P.J. Coelho, L.H. Melo de Carvalho, A. Samat, R. Guglielmetti, Helv. Chim. Acta 85 (2005) 442–450.
[5] (a) S.P.G. Costa, J. Griffiths, G. Kirsch, A.M.F. Oliveira-Campos, Ann. Quím. Int. Ed. 94 (1998) 186–188;
(b) V.A. Barachevsky, A.M.F. Oliveira-Campos, L.V. Stebunova, G.K. Chudinova, V.G. Avakyan, I.A. Maslianitsin, V.D. Shigorin, J. Sci. Appl. Photogr. (Russ.) 47 (2002) 4–8;
(c) M.M.M. Raposo, A.M.R.C. Sousa, A.M.C. Fonseca, G. Kirsch, Tetrahedron 61 (2005) 8249–8256.
[6] P.R. Prasad, D.J. Williams, Introduction to Nonlinear Optical Effects in Molecules and Polymers, Wiley-Interscience, New York, 1991.
[7] A.K. Jeewandara, K.M. Nalin de Silva, J. Mol. Struct. (Theochem.) 686 (2004) 131–136.
[8] A.D. Towns, Dyes Pigm. 42 (1999) 3–28.
[9] S.K. Yesodha, C.K. Sadashiva Pillai, N. Tsutsumi, Prog. Polym. Sci. 29 (2004) 45–74.
[10] P.-O. Åstrand, P. Sommer-Larsen, S. Hvilsted, P.S. Ramanujam, K.L. Bak, S.P.A. Sauer, Chem. Phys. Lett. 325 (2000) 115–119.
[11] M.G. Hutchings, P. Gregory, J.S. Campbell, A. Strong, J.-P. Zamy, A. Lepre, A. Mills, Chem. Eur. J. 3 (1997) 1719–1727.
[12] M.G. Hutchings, A. Mills, Dyes Pigm. 47 (2000) 23–31.
[13] G. McGeorge, R.K. Harris, A.M. Chippendale, J.F. Bullock, J. Chem. Soc., Perkin Trans. 2 (1996) 1733–1738.
[14] P.C. Miranda, L.M. Rodrigues, M.S.T. Gonçalves, S.P.G. Costa, R. Hrdina, A.M.F. Oliveira-Campos, Adv. Colour Sci. Technol. 4 (2001) 21–27.
[15] A.E.H. Machado, L.M. Rodrigues, S. Gupta, A.M.F. Oliveira-Campos, A.M.S. Silva, J. Mol. Struct. 738 (2005) 239–245.
[16] D.F. Eaton, Pure Appl. Chem. 60 (1988) 1107–1114.
[17] (a) J.J.P. Stewart, J. Comput. Chem. 10 (1989) 209–220;
(b) J.J.P. Stewart, J. Comput. Chem. 10 (1989) 221–264.
[18] AMPAC with Graphical User Interface, Version 8.16.5, Semichem Inc., Shawnee Mission, USA, 2005.
[19] M.J. Frisch, G.W. Trucks, H.B. Schlegel, G.E. Scuseria, M.A. Robb, J.R. Cheeseman, J.A. Montgomery Jr., T. Vreven, K.N. Kudin, J.C. Burant, J.M. Millam, S.S. Iyengar, J. Tomasi, V. Barone, B. Mennucci, M. Cossi, G. Scalmani, N. Rega, G.A. Petersson, H. Nakatsuji, M. Hada, M. Ehara, K. Toyota, R. Fukuda, J. Hasegawa, M. Ishida, T. Nakajima, Y. Honda, O. Kitao, H. Nakai, M. Klene, X. Li, J.E. Knox, H.P. Hratchian, J.B. Cross, V. Bakken, C. Adamo, J. Jaramillo, R. Gomperts, R.E. Stratmann, O. Yazyev, A.J. Austin, R. Cammi, C. Pomelli, J.W. Ochterski, P.Y. Ayala, K. Morokuma, G.A. Voth, P. Salvador, J.J. Dannenberg, V.G. Zakrzewski, S. Dapprich, A.D. Daniels, M.C. Strain, O. Farkas, D.K. Malick, A.D. Rabuck, K. Raghavachari, J.B. Foresman, J.V. Ortiz, Q. Cui, A.G. Baboul, S. Clifford, J. Cioslowski, B.B. Stefanov, G. Liu, A. Liashenko, P. Piskorz, I. Komaromi, R.L. Martin, D.J. Fox, T. Keith, M.A. Al-Laham, C.Y. Peng, A. Nanayakkara, M. Challacombe, P.M.W. Gill, B. Johnson, W. Chen, M.W. Wong, C. Gonzalez, J.A. Pople, Gaussian 03, Revision D. 01-SMP, Gaussian Inc., Pittsburgh, PA, 2004.
[20] (a) A.D. Becke, J. Chem. Phys. 98 (1993) 5648–5652;
(b) C. Lee, W. Yang, R.G. Parr, Phys. Rev. B 37 (1988) 785–789.
[21] (a) K.D. Dobbs, W.J. Wehre, J. Comput. Chem. 8 (1987) 880–893;
(b) K.D. Dobbs, W.J. Wehre, J. Comput. Chem. 7 (1986) 359–378;
(c) M.J. Frisch, J.A. Pople, J.S. Binkley, J. Chem. Phys. 80 (1984) 3265–3269.
[22] M.J.S. Dewar, E.G. Zoebisch, E.F. Healy, J.J.P. Stewart, J. Am. Chem. Soc. 107 (1985) 3902–3909.
[23] D.A. Kleinman, Phys. Rev. 126 (1962) 1977–1979.
[24] (a) M.E. Casida, in: D.P. Chong (Ed.), Recent Advances in Density Functional Methods, vol. 1, World Scientific, Singapore, 1995, p. 155;
(b) E.K.U. Gross, C.A. Ullrich, U.J. Gossmann, Density Functional Theory of Time-Dependent Systems, vol. 337, Plenum, New York, 1995, p. 149, NATO ASI Ser. B.
[25] W. Koch, M.C. Holthausen, A Chemist's Guide to Density Functional Theory, 2nd ed., Wiley–VCH, Weinheim, Fed. Rep. Germany, 2001.
[26] (a) J.B. Foresman, M. Head-Gordon, J.A. Pople, M.J. Frisch, J. Phys. Chem. 96 (1992) 135–149;
(b) J. Paldus, X. Li, Adv. Chem. Phys. 110 (1999) 1–176.
[27] K. Clays, A. Persoons, Rev. Sci. Instrum. 63 (6) (1992) 3285–3289.
[28] P.L. Franzen, S.C. Zilio, A.E.H. Machado, L.T. Ueno, J.M. Madurro, A.G. Brito-Madurro, R.N. Sampaio, N.M. Barbosa Neto, J. Mol. Struct., Submitted for publication.
[29] K. Clays, A. Persoons, L. de Maeyer, Modern nonlinear optics. Part 3, Adv. Chem. Phys. Series 85 (1994) 455–498.
[30] H. Rau, in: H. Dürr, H. Bouas-Laurent (Eds.), Studies in Organic Chemistry 40: Photochromism, Molecules and Systems, Elsevier, Amsterdam, 1990, chap. 4.
[31] A.E.H. Machado, D. Severino, J. Ribeiro, R. De Paula, M.H. Gehlen, H.P.M. Oliveira, M.S. Matos, J.A. Miranda, Photochem. Photobiol. Sci. 3 (2004) 79–84.
[32] P. Likowski, A. Koll, A. Karpfen, P. Wolschann, Chem. Phys. Lett. 370 (2003) 74–82.
[33] J. Seixas de Melo, R.S. Becker, A.L. Maçanita, J. Phys. Chem. 98 (1994) 6054–6058.
[34] A.B.J. Parusel, G. Kökler, S. Grimme, J. Phys. Chem. A 102 (1998) 6297–6306.
[35] A.B.J. Parusel, Chem. Phys. Lett. 340 (2001) 531–537.
[36] J.L. Oudar, J. Chem. Phys. 67 (1977) 446–457.
[37] G.L.C. Moura, A.M. Simas, J. Miller, Chem. Phys. Lett. 257 (1996) 639–646.
[38] D.C. Harris, M.D. Bertolucci, Symmetry and Spectroscopy: An Introduction to Vibrational and Electronic Spectroscopy, Dover, New York, 1989.
[39] A. Gilbert, J. Baggott, Essentials of Molecular Photochemistry, Blackwell, London, 1991.
[40] N.J. Turro, Modern Molecular Photochemistry, University Science Books, USA, 1991.
[41] J.R. Lakowicz, Principles of Fluorescence Spectroscopy, 2nd ed., Kluwer Academic/Plenum Publishers, New York, 1999.
[42] C. Reichardt, Chem. Rev. 94 (1994) 2319–2358.
[43] B.A. Sriyanka Mendis, K.M.N. de Silva, J. Mol. Struct. (Theochem.) 678 (2004) 31–38.
[44] (a) H.A. Kurtz, J.J.P. Stewart, K.M. Dieter, J. Comput. Chem. 11 (1990) 82–87;
(b) M.J.S. Dewar, J.J.P. Stewart, Chem. Phys. Lett. 111 (1984) 416–420.
[45] A.M.S. Silva, G.B. da Rocha, P.H. Menezes, J. Miller, A.M. Simas, J. Braz. Chem. Soc. 16 (2005) 583–588.
[46] P.A. Fantin, P.L. Barbieri, A. Canal Neto, F.E. Jorge, J. Mol. Struct. (Theochem.) 810 (2007) 103–111.
[47] (a) D. Xenides, J. Mol. Struct. (Theochem.) 804 (2007) 41–46;
(b) G. Maroulis, J. Chem. Phys. 108 (1998) 5432–5448;
(c) D. Xenides, G. Maroulis, Chem. Phys. Lett. 319 (2000) 618–624;
(d) G. Maroulis, D. Xenides, J. Phys. Chem. A 107 (2003) 712–719;
(e) G. Maroulis, J. Chem. Phys. 118 (2003) 2673–2687.
[48] A.F. Marks, A.K. Noah, M.R.V. Sahyun, J. Photochem. Photobiol. A 139 (2001) 143–149.
[49] F. Babudri, A.R. Cicciomessere, G.M. Farinola, V. Fiandanese, G. Marchese, R. Musio, F. Naso, O. Sciacovelli, J. Org. Chem. 62 (1997) 3291–3298.
[50] S.K. Stewart, A. Whiting, Tetrahedron Lett. 36 (1995) 3925–3928.
[51] M.A. Pauley, H-W. Guan, C.W. Wang, A.K.-Y. Jen, J. Chem. Phys. 104 (1996) 7821–7829.
[52] F.L. Huyskens, P.L. Huyskens, A.P. Persoons, J. Chem. Phys. 108 (1998) 8161–8171.